JLAB-TN-00-000
GlueX-doc-1660
Version 0.1
January 04,2011

Calculation of Radiation Damage to Silicon Photomultipliers in GlueX Experiment

P. Degtiarenko, A. Fassò, G. Kharashvili, A. Somov

Abstract

Understanding the effects of neutron radiation is critical for operation of silicon photomultipliers, the photodetectors which are planned to be used in the barrel electromagnetic calorimeter and the time-of-flight Start Counter detector of the GlueX experiment. Neutron radiation damage and dose equivalent rates were computed using two independent simulation packages: FLUKA and GEANT3.

1 Introduction

Silicon photomultipliers (SiPM) are a relatively new type of photodetector currently being used in various experiments in nuclear and high energy physics. Most characteristics of SiPMs, such as a timing resolution, quantum efficiency and gain, are comparable with that of traditional PMTs. However, the ability to operate SiPMs in large magnetic fields makes these photodetectors attractive for many applications in calorimetry and time-of-flight measurements.

In the GlueX experiment at Jefferson Lab, SiPMs are planned to be used as photodetectors for the barrel electromagnetic calorimeter (BCAL) and the time-of-flight Start Counter (SC) detector. Both, the BCAL and the SC will be positioned inside a 2.2 T solenoid magnet. The BCAL is a 3.9 m long cylindrical detector with the inner and outer radii of 65 and 90 cm, respectively. It is made of 180 layers of lead sheets and scintillator fibers placed in lead grooves between the layers. The BCAL is divided into 48 sectors (modules), each of which is

organized into 40 readout blocks. Light from scintillator fibers of each block will be detected from both sides of the BCAL by a 4×4 array of SiPMs. The effective area of the SiPM array is $1.2 \times 1.2\ cm^2$.

The SC is a cylinder-shaped detector consisting of 40 scintillator paddles positioned around the GlueX liquid hydrogen target. Light produced in the scintillator is detected from the upstream side of each paddle by an array of SiPMs.

Recent radiation tests of SiPMs performed at Jefferson Lab [1] showed a relatively large sensitivity of these photodetectors to neutron radiation. Specifically, an accumulated dose of 32 rem from an AmBe neutron source increased the dark current of Hamamatsu SiPMs by a factor of 4.4. Similar behavior of the dark current was observed when the SiPMs were exposed to neutron radiation in experimental Hall-A.

In order to estimate the degradation of the BCAL and SC SiPM's performance in the Hall-D, we performed a detailed simulation of the neutron background using a Geant program provided by the JLab radiation control (RadCon) group and a FLUKA program. The SiPM dark current increase can be estimated by comparing neutron doses predicted by the simulations with that acquired during the radiation tests. The RadCon Geant is based on the standard Geant 3 but includes a better description of the photo/electro-nuclear processes.

During the SiPM radiation tests, neutron doses were measured by a neutron survey meter. The neutron survey meter measures the so-called equivalent dose in units of rem, which accounts for different biological effects to tissue of different types of ionization. The neutron flux and energy can be translated to the equivalent dose using a biological damage coefficients curve presented in the upper plot of Fig. 1. Damage effects to Silicon detector caused by different particle types (which lead to the displacement of atoms in the crystal lattice and are associated with the kinetic energy releases to matter) can be characterized by a damage function presented in the bottom plot of Fig. 1. The curves on this plot correspond to different particle types and are normalized to an equivalent damage of 1 MeV neutrons. The shape of the biological damage coefficients curve of neutrons is somewhat similar to that of the damage function in Silicon. In order to compare damage effects to Silicon caused by different particle types with different energies, it is convenient to convert the particle fluence to the equivalent fluence of 1-MeV neutrons using the damage function presented in Fig. 1.

This note is organized as follows: in Section 2 we will describe the Monte-Carlo detector simulations and some physics models included into the Geant and FLUKA programs. The simulation results will be presented and discussed in Sections 3 and 4.

2 Monte-Carlo Modeling

The main goal of the GlueX experiment is to search for mesons with exotic-quantum-numbers in interactions of a linearly polarized photon beam with a 30 cm long liquid hydrogen target. The high-intensity photon beam will be produced via the Bremsstrahlung process by a 12 GeV electron beam incident on a thin diamond radiator. In order to increase the fraction of linearly

polarized photons, the photon beam is passed through a 3.4 mm diameter collimator. The flux of the collimated photons is about a $3.4 \cdot 10^9$ γ/sec in the beam energy range 1.2 MeV $< E_\gamma <$ 12 GeV, corresponding to a total beam power of about 0.7 W on the target. The energy spectrum of the collimated beam photons is presented in Fig. 2. The coherent peak in the energy spectrum between 8.4 GeV $< E_\gamma <$ 9.0 GeV represents the photon beam energy range of interest used for the search of exotic mesons. The degree of linear polarization in this energy region is 40%. The low-energy part of the energy spectrum can be relatively well parametrized by a 1/E function. The energy spectrum from Fig. 2 was used as an input for both Geant and FLUKA simulations.

The official GlueX detector simulation is based on Geant 3.21. The Geant geometry contains a detailed description of the GlueX detector and is presented in the top plot of Fig. 3. In order to verify neutron fluences predicted by Geant we compared particle distributions inside the detector using the FLUKA simulation. In the FLUKA simulation we used a simplified GlueX geometry, that is expected to represent reasonably well the detector material and major sources of particle scattering. The FLUKA geometry is shown in the bottom plot of Fig. 3. The geometries of the gaseous detectors (the Central Drift Chambers (CDC) and the Forward Drift Chambers (FDC)) have been greatly simplified relative to their full description in Geant. The main geometry simplifications are listed below:

- The Central Drift Chamber was modeled as a tube filled with an admixture of 85% Ar and 15% CO_2 gases. 24 layers of CDC straw tubes containing wires were grouped into 3 rings. The thickness and equivalent material of each ring corresponded to that of 8 straw layers. Two rings were placed at the inner and outer radii of the CDC layers corresponding to 9 cm and 55.6 cm, respectively, and the third ring was positioned in between them. The CDC geometry contains two endplates situated at the upstream and downstream ends of the gas volume.

- The Forward Drift Chamber consists of 4 packages positioned at different z coordinates inside the solenoid magnet. Each package contains 6 cathode-wire-cathode sandwich chambers filled with an $ArCO_2$ gas. The geometry of each package in FLUKA was modeled as four tube-shaped volumes. The volumes were filled with an average material and represented the following parts of the chambers: (1) the FDC ground plates made of Aluminized Mylar; (2) the gas volumes; (3) the outer part of cathode plates with the inner radius of 1.3 cm made of Kapton and covered with Copper; (4) the inner part of cathode plates made of Kapton and positioned inside the photon beamline with the outer radius of 1.3 cm. We also implemented into the geometry volumes corresponding to frames of the FDC chambers and FDC cables going from from each package to the upstream end of the CDC chamber. The frames were modeled as cylinders with the inner and outer radii of 51 cm and 53 cm, respectively made of a composite material consisting of 70% Borosilicate Glass and 30% Epoxy Resin. The FDC cables were simulated as a cylinder made of PVC and Copper with inner and outer radii of 62.5 cm and 62.61 cm, respectively.

- The geometry of a Cerenkov gaseous detector was simplified to a tube filed with C_4D_{10} gas and positioned after the solenoid magnet. Detector mirrors were not included into the geometry.

- The field map of the solenoid magnet implemented in the Geant simulation was obtained using a TOSCA magnetic field simulation package [2]. The B_z component of the magnetic field for different radial distances from the beamline as a function of the Z-coordinate is presented in Fig. 4. As can be seen, the value of B_z is almost independent of the radial distance from the beamline, r. Therefore, in the FLUKA simulation we neglected the field dependence on the radial distance and implemented the B_z shape from Fig. 4 corresponding to $r = 0$. The magnetic field shape was parametrized using a polynomial function.

2.1 GEANT

The Geant simulation provided by the Radiation Control group represents the standard Geant3 with a better description of photo/electro-nuclear interactions. The modifications to the standard GEANT3 include replacement of the 'PFIS' (photofission) mechanism with the photonuclear absorption mechanism in accordance with total photonuclear cross sections and invoking a nuclear fragmentation event generator, DINREG, to produce secondary hadrons in these interactions. The code DINREG was developed by Pavel Degtiarenko and Mikhail Kossov. The generator is exclusive, meaning that it generates fragmentation events fully conserving 4-momentum, baryon number and charge in the reaction.

Another modification is the new process of electro-nuclear interaction which assumes that the mostly low-Q2 interactions of electrons with nuclei can be described in terms of the Equivalent Photon Approximation (EPA), using real photon cross sections for the equivalent photons and then modeling the interaction analogous to the gamma-nucleus process. The electron interactions are modeled as interaction of the flux of equivalent photons along each electron step in the cascade. No high-Q2 processes are thus modeled, assuming all electron interaction is energy loss in forward direction. This approximation is good enough for practical purposes of bulk background calculations, but of course fails to describe details of large angle, deep inelastic electron scattering, as well as the quasielastic electron scattering off nuclei. The results should be accurate within factor 2-3 in general, may be worse for very forward hadron production. The electron scattering at large angles could be underestimated.

The code is used extensively at JLab for background and shielding calculations, as the photoneutrons contribute significantly to radiation background problems at CEBAF. No detailed reference with the description of the GEANT/DINREG code system exists. DINREG was described in an ITEP preprint [3] and not published later; there are several papers referring to the results of its use, mostly in detector acceptance calculations [4]. Ref. [5] describes the use of the GEANT/DINREG model in shielding calculations at CEBAF.

The new, completely rewritten in c++ by M. Kossov, version of the Monte Carlo (named

CHIPS) is included in the new Geant4 package, with proper model description and benchmark tests [6].

2.2 FLUKA

FLUKA [7, 8] is a multi-purpose Monte Carlo code for particle transport and interactions, which is capable of simulating all components of hadronic and electromagnetic cascades from very high energies down to thermal neutrons. Its predictive power has been confirmed by a large number of benchmarking studies, comparing FLUKA results against experimental data. The code is provided with a number of statistical tools (biasing options) to reduce the variance of the results.

FLUKA is used in a large number of very different applications: accelerator shielding and activation, dosimetry and radiation protection, calorimetry, cosmic ray research, hadron therapy, etc. A further common application is to predict radiation damage.

The probability for a displacement damage to occur due to non-ionizing energy loss (NIEL) is calculated by scoring the 1-MeV neutron equivalent fluence of all particles in the regions of interest, weighted with published damage cross sections [9]. The probability of single event upsets (SEU) is calculated using the fluence of particles with energies >20 MeV and the available SEU cross section data [10].

2.2.1 The FLUKA physics models

Several different models are used by FLUKA to simulate particle transport and interactions. Charged particle transport is based on Bethe-Bloch ionization and Moliere multiple scattering, including some higher order corrections. It is possible to transport charged particles in magnetic fields described by the user. Electron, positron and photon electromagnetic interactions include bremsstrahlung, positron annihilation at rest and in flight, Rayleigh and Compton scattering on bound electrons, fluorescence, Auger and pair production; in all these interactions the energy and angle of the secondaries are fully correlated.

The physical interaction models of interest for the present Note concern the hadronic and the photonuclear interactions. The PEANUT event generator is based on different models describing hadron inelastic interactions depending on energy: Glauber-Gribov cascade with formation zone, Generalized IntraNuclear Cascade (GINC), preequilibrium stage with current exciton configuration and excitation energy, evaporation (or Fermi break-up or fission), and gamma de-excitation.

Photonuclear reactions at different photon energies are Giant Resonance, Quasideuteron, Delta Resonance and Vector Meson Dominance with shadowing. The total interaction cross section is tabulated or parametrized according to experimental data. The nuclear de-excitation and emission of secondaries are handled by the hadronic event generators listed above.

3 Results

We have compared fluences of different particle types in the BCAL SiPM region predicted by the Geant and FLUKA simulations. The particle fluences were averaged over a ring with the inner and outer radii of 65 cm and 90 cm from the beamline, respectively. In the Geant simulation, the ring was positioned 75 cm downstream from the downstream edge of the BCAL. In the FLUKA simulation particle fluences were also estimated in a ring placed after the BCAL light guides, about 15 cm from the BCAL edge. Spectra of different particle types obtained with the Geant and FLUKA simulations are presented in Fig. 5. The particle spectra were found to be in a relatively good agreement between the Geant and FLUKA simulations. The difference in neutron fluences between Geant and FLUKA was found to be smaller than a factor of two for neutrons with a kinetic energy larger than 0.1 MeV, i.e., in the energy range where damage to Silicon dominates.

The fluences of all particles inside the GlueX detector obtained using the FLUKA simulation were scaled to a 1-MeV neutron equivalent fluence in Silicon using the damage function coefficients from Fig. 1. The 1-MeV neutron equivalent fluences of all particles and neutrons only are presented in Fig. 6. As can be seen, the 1-MeV equivalent fluence in the SiPM region is dominated by the neutron background. Other types of background particles, which originate mostly inside the GlueX target, are shielded by the BCAL material. The 1-MeV equivalent fluence of neutrons in the BCAL SiPM region is listed in Table 1. The FLUKA simulation predicts the neutron background to be 18.0 $n_{eq} \cdot sec^{-1} \cdot cm^{-2}$ after the BCAL light guides and 16.9 $n_{eq} \cdot sec^{-1} \cdot cm^{-2}$ 75 cm downstream from the BCAL edge. These numbers can be compared with the neutron fluence of 30.5 $n_{eq} \cdot sec^{-1} cm^{-2}$ estimated with the Geant simulation 75 cm downstream from the BCAL.

1-MeV neutron equivalent particle fluence distributions in the experimental Hall-D estimated with the FLUKA simulation are presented in Fig. 7. The corresponding dose equivalent rate is shown in Fig. 8.

Simulation Type	n	p	π	e^-	e^+	Total
FLUKA SiPM	18.0	1.7	1.8	1.0	0.2	22.9 ± 0.2
FLUKA 75 cm downstream	16.9					
Geant 75 cm downstream	30.5					

Table 1: 1-MeV neutron equivalent fluence in units of $n_{eq} \cdot sec^{-1} \cdot cm^{-2}$ estimated with FLUKA and Geant simulations. The fluences were computed in the SiPM region after the BCAL light guides and 75 cm downstream from the BCAL.

4 Discussion

We have estimated background in the BCAL SiPM region using two independent simulation programs: the RadCon Geant3 and the FLUKA. The background was computed in units of a 1-MeV neutron equivalent fluence in Silicon. This unit can be used to characterized the damage to the Silicon detectors caused by different particle types. The background in the SiPM region was found to be dominated by neutrons, except for the SiPMs, positioned at the radial distance closest to the beamline. These SiPMs are less shielded from the background particles originated inside the GlueX target by the BCAL material and are exposed to radiation damage from other particle types comparable to that from neutrons. Neutron fluences predicted by Geant and FLUKA simulations were compared 75 cm downstream from the BCAL edge. The fluences were found to be 30.5 $n_{eq} \cdot sec^{-1} \cdot cm^{-2}$ and 16.9 $n_{eq} \cdot sec^{-1} \cdot cm^{-2}$, respectively. The Geant and FLUKA results are considered to be in satisfactory agreement. The discrepancy is due to:

1. Different physics models of photo-nucleus interactions used in Geant and FLUKA simulations.

2. Simplified GlueX detector geometry used in the FLUKA simulation.

According to the irradiation tests of BCAL SiPMs performed at JLab in the experimental Hall-A and using an AmBe neutron source, the dark current of the photodetectors is expected to be increased by about a factor of 5 for the accumulated neutron 1-MeV equivalent fluence between $0.8 - 1.9 \cdot 10^9$ $n_{eq} \cdot cm^{-2}$ [1]. That fluence corresponds to the continuous operation of the BCAL SiPMs for about 1-2 years assuming a background of 30.5 $n_{eq} \cdot sec^{-1} cm^{-2}$.

The 1-MeV neutron equivalent fluence in the Start Counter SiPM region was estimated to be comparable with the average fluence in the BCAL SiPM region. Meanwhile, the dark current increase in the Start Counter SiPM is expected to be less critical for the time-of-flight measurements [].

References

[1] Neutron radiation tests performed by Yi Qiang `hhttp://www.jlab.org/Hall-D/software/wiki/index.php/SiPM_Radiation_Hardness_Test`.

[2] D. Lawrence and S. Taylor, "Track Finding and Fitting in GlueX: Development Report", GlueX-doc-1004, (2008).

[3] P. V. Degtyarenko et al., "Inelastic Electron-Nucleus Interactions at 5 GeV detected by ARGUS", Z.Phys.A, **335**, 231-238 (1990).

[4] P. V. Degtyarenko and M. V. Kossov, "Monte Carlo program for nuclear fragmentation", Preprint ITEP-11, 1-18 (1992). P. V. Degtyarenko et al., "Multiple hadron production by

14.5 GeV electron and positron scattering from nuclear targets", Phys.Rev.C, **50**, R541-R545 (1994).

[5] P. V. Degtyarenko, "Applications of the Photonuclear Fragmentation Model to Radiation Protection Problems", Proceedings of SATIF2, 12-13 October 1995 CERN, Geneva, Switzerland.

[6] P. V. Degtyarenko, M. V. Kossov, H-P. Wellisch, "Chiral Invariant Phase Space Event Generator I. Nucleon-antinucleon annihilation at rest", Eur. Phys. J. A **8**, p.217-222 (2000). P. V. Degtyarenko, M. V. Kossov, H-P. Wellisch, "Chiral Invariant Phase Space Event Generator II. Nuclear pion capture at rest and photonuclear reactions below the $\Delta(3,3)$ resonance", Eur. Phys. J. A **9**, p.411-420 (2000). P. V. Degtyarenko, M. V. Kossov, H-P. Wellisch, "Chiral Invariant Phase Space Event Generator III. Modeling of real and virtual photon interactions with nuclei below pion production threshold", Eur. Phys. J. A **9**, p.421-424 (2000).

[7] A. Fasso', A. Ferrari, J. Ranft, and P.R. Sala, "FLUKA: a multi-particle transport code" CERN-2005-10 (2005), INFN/TC_05/11, SLAC-R-773.

[8] G. Battistoni, S. Muraro, P.R. Sala, F. Cerutti, A. Ferrari, S. Roesler, A. Fasso', J. Ranft, "The FLUKA code: Description and benchmarking" Proceedings of the Hadronic Shower Simulation Workshop 2006, Fermilab 6-8 September 2006, M. Albrow, R. Raja eds., AIP Conference Proceeding 896, 31-49, (2007).

[9] M. Huhtinen, and P.A. Aarnio, "Pion induced displacement damage in silicon devices". Nuclear Instruments and Methods A335, 580-582 (1993).

[10] G.P. Summers, et al., "Damage correlations in semiconductors exposed to gamma, electron and proton radiations". IEEE Trans. Nucl. Sci. 40, 1372-1379 (1993).

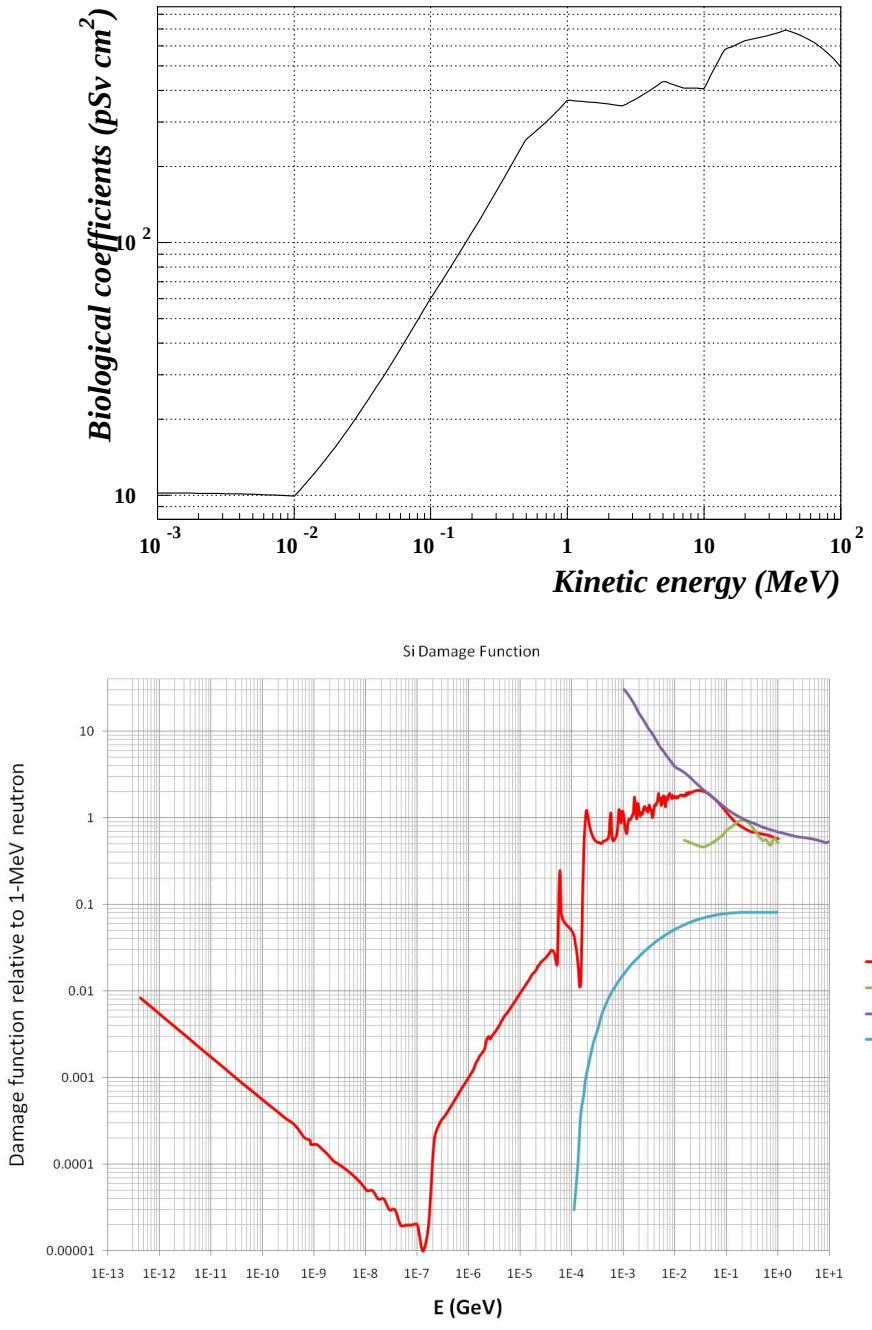

Figure 1: Biological damage conversion coefficients for neutrons (top). Effective damage to Silicon detector relative to 1-MeV neutron caused by different particle types (bottom).

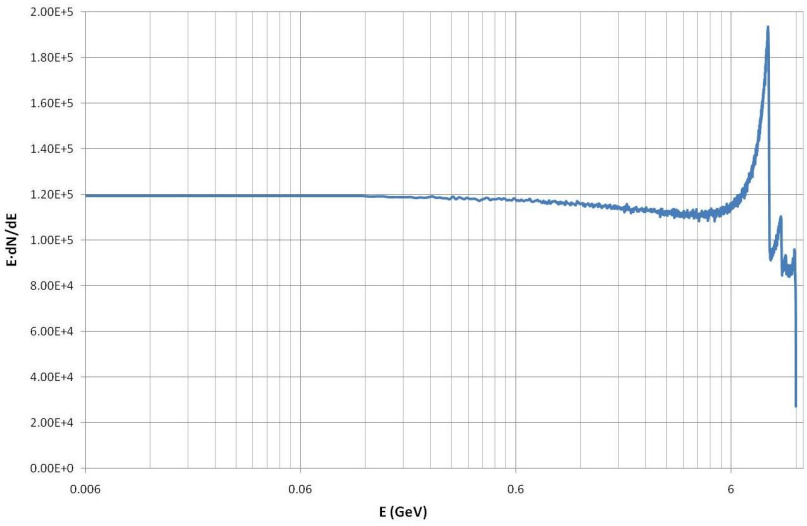

Figure 2: Energy spectrum of the GlueX photon beam after the collimator. This spectrum was used as an input for Geant and FLUKA simulations.

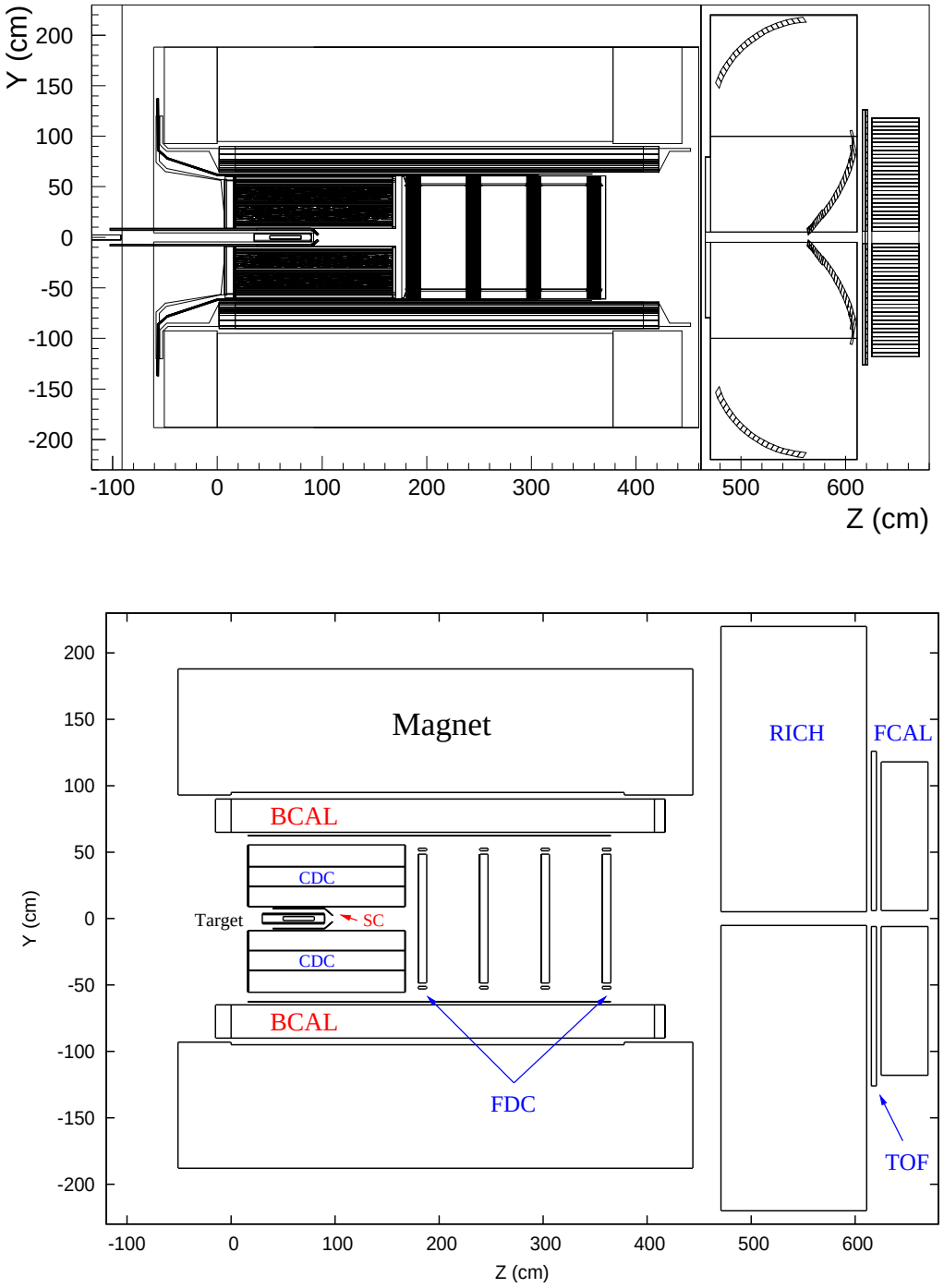

Figure 3: Plane view of the GlueX detector geometry implemented into Geant (top) and FLUKA (bottom) simulations. GlueX sub-detectors are: Target, Start Counter (SC), Barrel Electromagnetic Calorimeter (BCAL), Central Drift Chamber (CDC), Forward Drift Chamber (FDC), Rich Cerenkov counter (RICH), Time-of-Flight counter (TOF), and Forward Electromagnetic Calorimeter (FCAL).

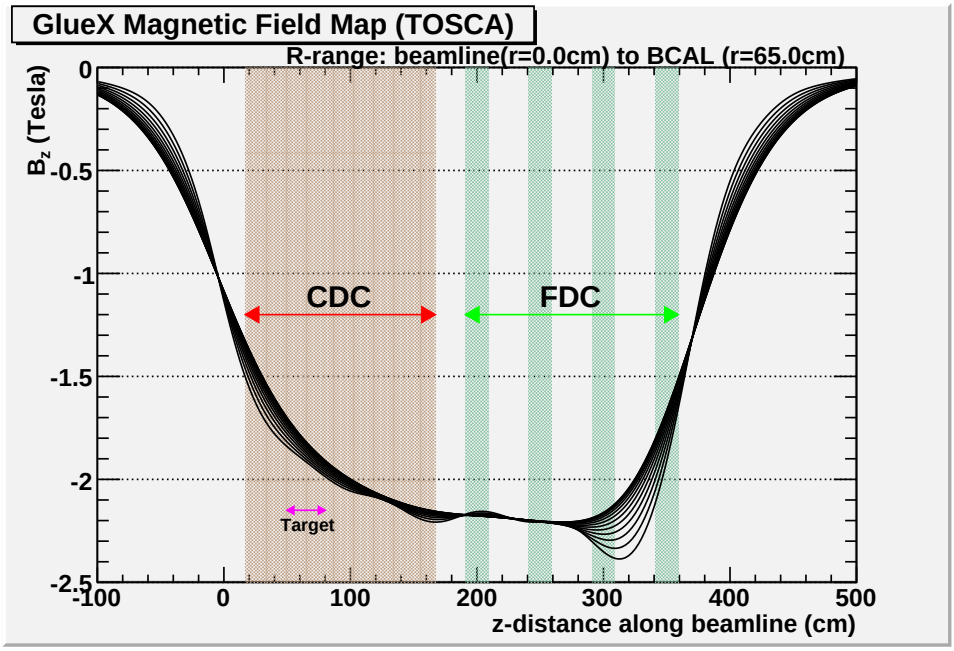

Figure 4: Magnetic field distribution inside the GlueX solenoid magnet obtained using TOSCA magnetic field simulation package.

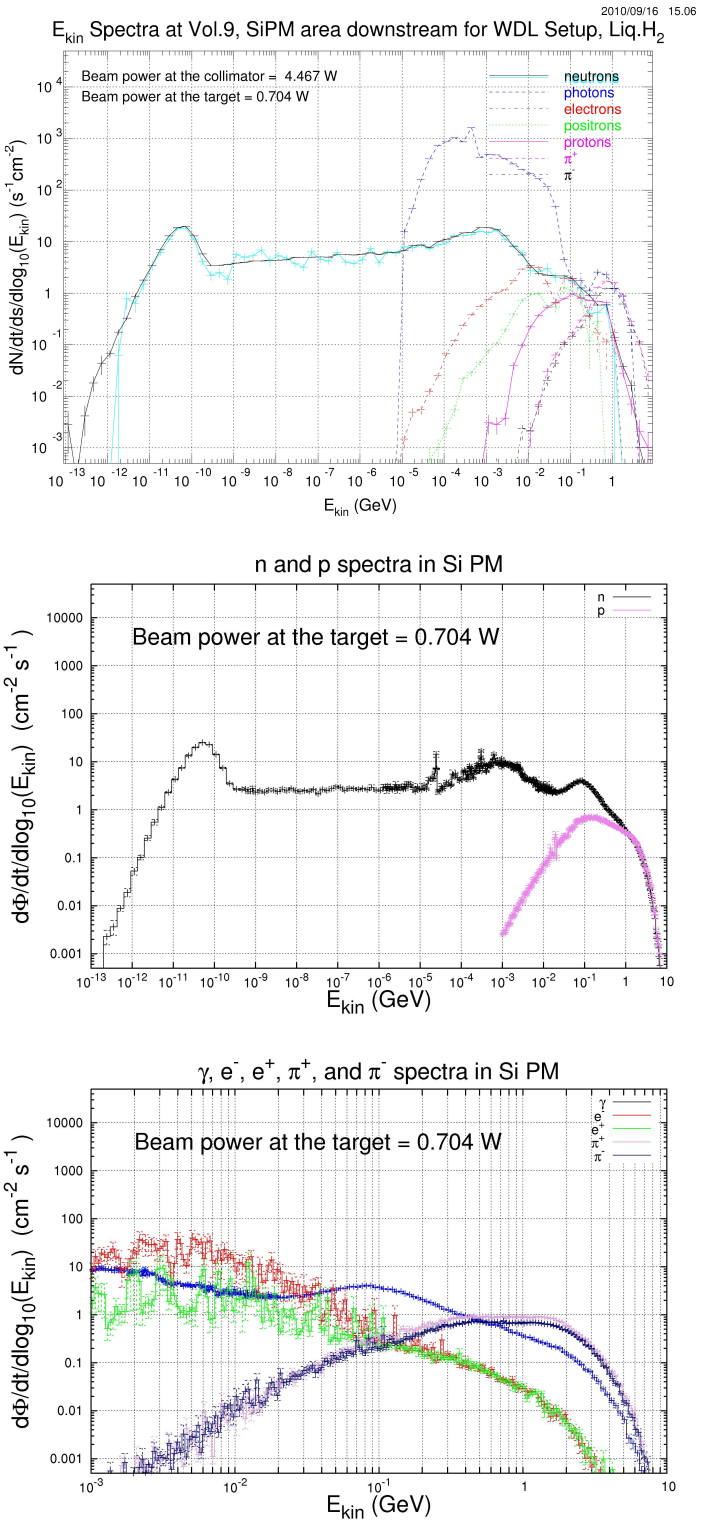

Figure 5: Particle spectra computed with the RadCon Geant in the SiPM region (top). Corresponding particle fluences of neutrons and protons (middle) and other particle types (bottom) predicted by FLUKA simulation.

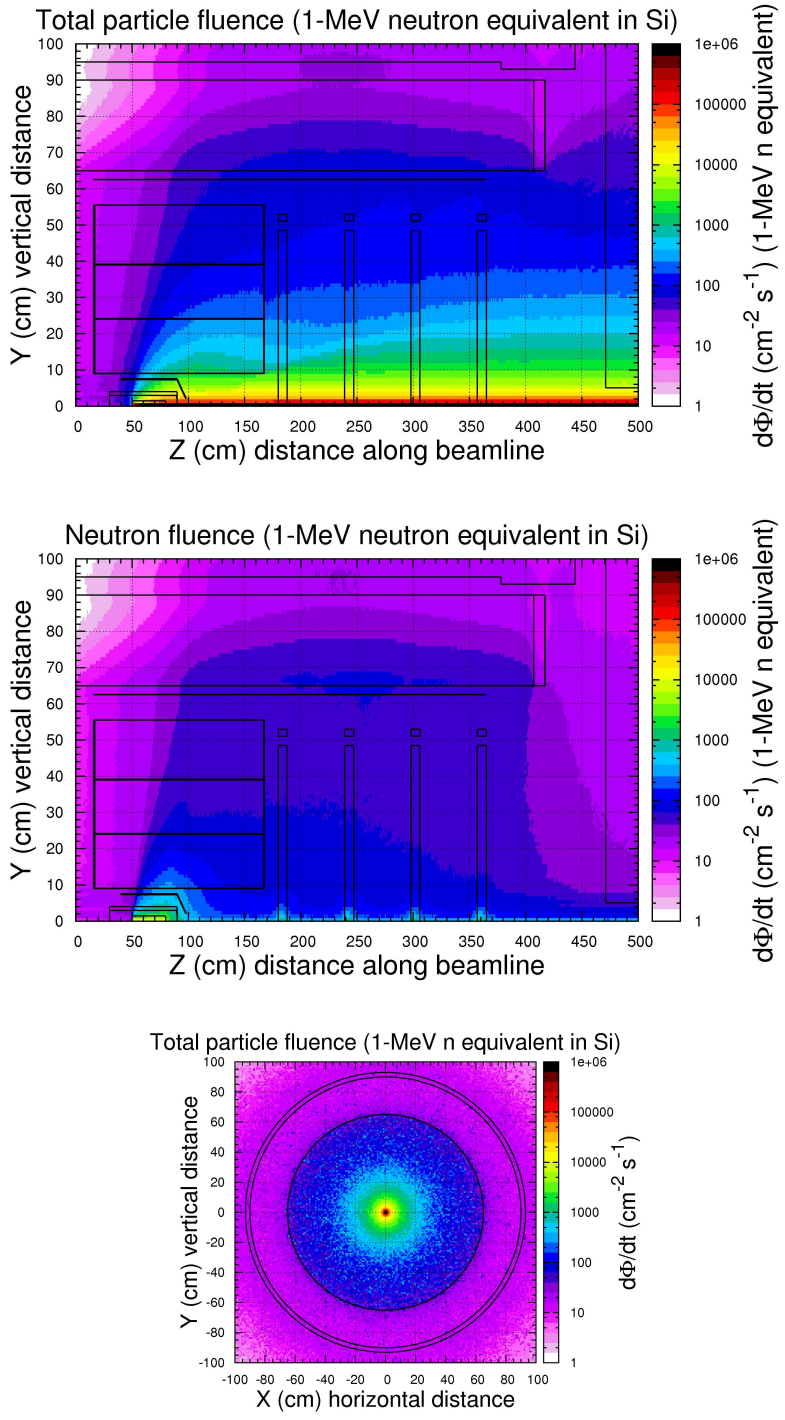

Figure 6: Total particle fluence (top) and neutron fluence (middle) inside the GlueX detector in 1-MeV neutron equivalent obtained with the FLUKA simulation. X-Y distribution of the particle fluence in the BCAL SiPM region is presented in the bottom plot.

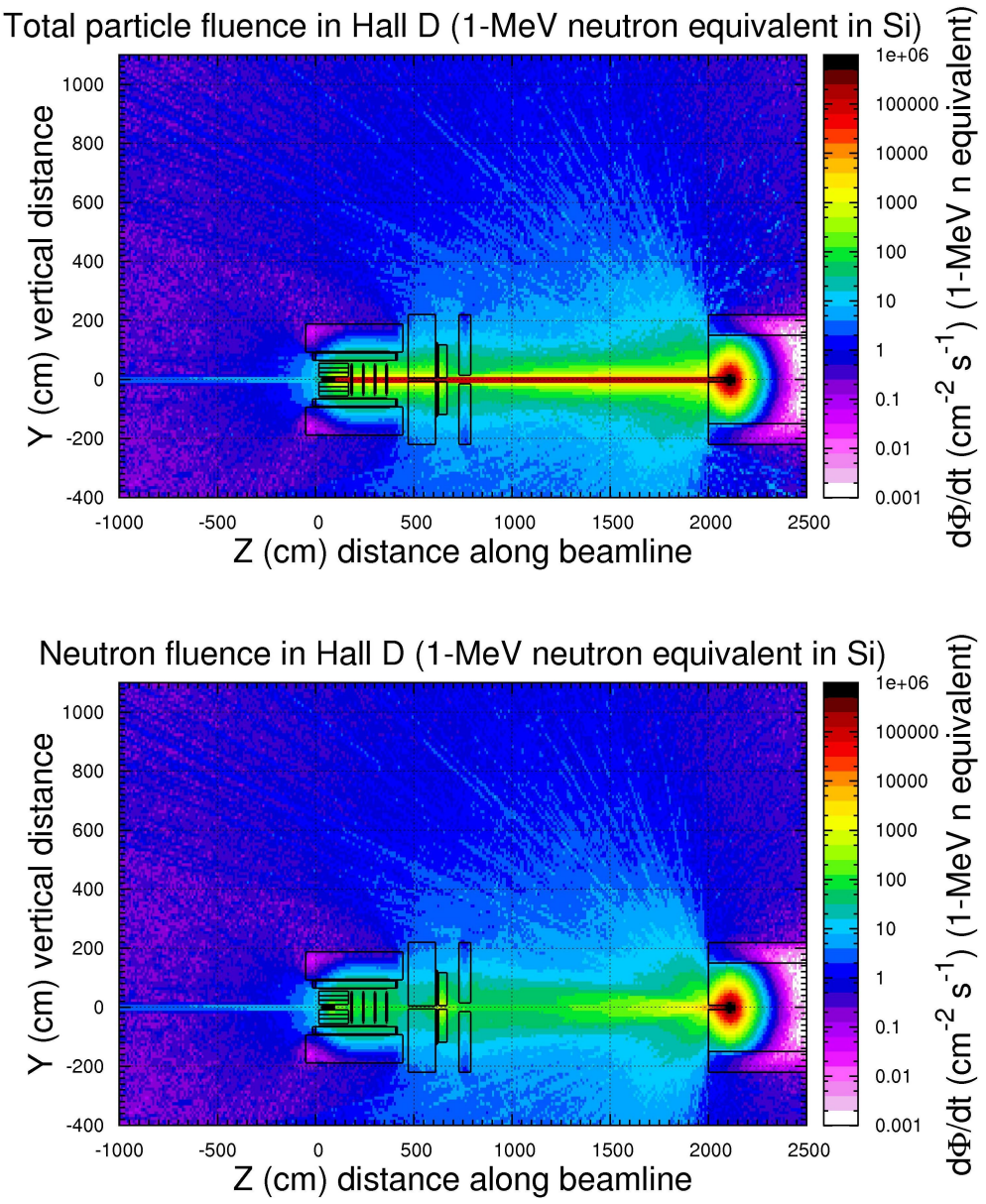

Figure 7: 1-MeV neutron equivalent in Silicon fluences of all background particles (top) and neutrons (bottom) in the experimental Hall-D estimated with FLUKA simulation.

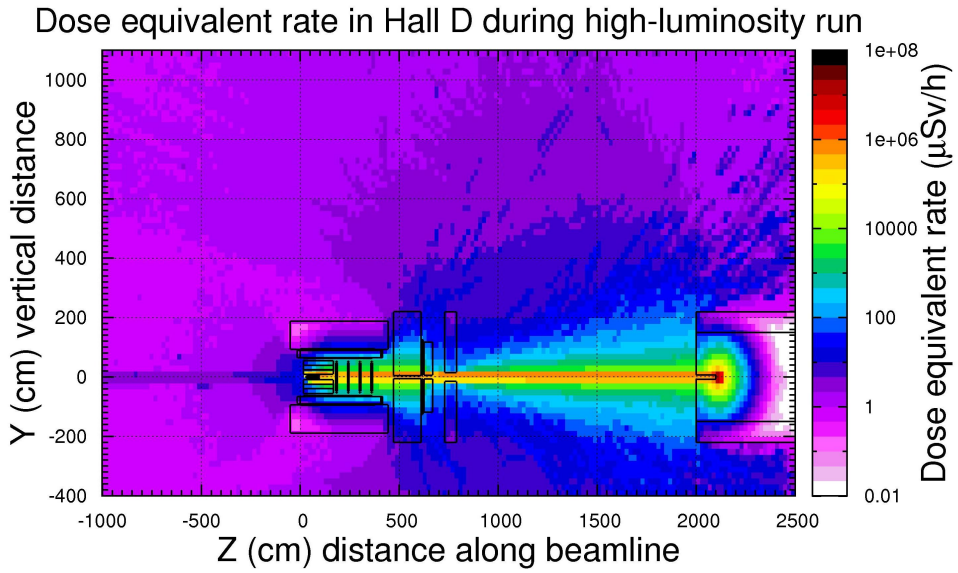

Figure 8: Dose equivalent rate in the experimental Hall-D estimated with FLUKA simulation.